Received: 19 June 2020 | Revised: 5 November 2021 | Accepted: 6 January 2022

DOI: 10.1111/jfr3.12787

ORIGINAL ARTICLE

CIWEM Chartered Institution of Water and Environmental Management | Journal of Flood Risk Management | WILEY

# Improving hydrological climate impact assessments using multirealizations from a global climate model

**Frederiek Sperna Weiland**[1] | **Dana Stuparu**[1] | **Renske de Winter**[1] | **Marjolijn Haasnoot**[1,2]

[1]Deltares, Delft, the Netherlands

[2]Department of Physical Geography, Utrecht University, Utrecht, the Netherlands

**Correspondence**
Frederiek Sperna Weiland, Unit Inland Water Systems, Deltares, Boussinesqweg 1, 2629 HV, Delft, the Netherlands.
Email: frederiek.sperna@deltares.nl

**Funding information**
Deltares

**Abstract**

Many flood risk assessments account for uncertainties in future anthropogenic emissions by considering multiple representative concentration pathways (RCPs). The imperfect knowledge and representation of the climate system is considered with multiple global climate models (GCMs). Yet, uncertainty introduced by incomplete representation of natural variability is also relevant but not always accounted for. A set of realizations provides improved insights in natural variability presented by the GCM. This study explores the potential of using a set of realizations from a single GCM-RCP combination instead of single realizations. We use (subsets of) 16 realizations from EC-Earth for RCP8.5 and focus on three locations along the Rhine. We use a single GCM-RCP combination to avoid the interference of additional sources of uncertainty. We find that projected changes in future river flows highly depend on the realization chosen. Individual ensemble members provide different changes for annual mean flow, extreme flows, and regime shift. By increasing the number of realizations and combining their annual maxima in extreme value analysis, future projections of flow extremes converge. We conclude that a single ensemble realization gives overconfident and possibly erroneous projections. In climate science, this is well studied; however, in flood risk assessments, it is still often neglected.

**KEYWORDS**

climate change, flood risk, GCM, natural climate variability, Rhine

## 1 | INTRODUCTION

Climate change will affect the frequency and intensity of river floods worldwide (Alfieri et al., 2018; Forzieri et al., 2016; IPCC, 2014; van der Wiel et al., 2019; Whitfield, 2012). The assessment of climate change on future flood risk typically involves the following steps: (a) use global climate model or regional climate model (GCM or RCM) projections to simulate river flow changes, (b) extreme value analysis for the derivation of flood extremes for two or more future time-slices of at least 30 years, and (c) flood inundation modeling to assess impacts (Felder et al., 2018; Kay et al., 2020; Ward et al., 2012).

Projections of future changes in flood risk are one of the most challenging areas of climate change sciences and the spread of possible outcomes is large (DEFRA, 2012). Uncertainties arise from (at least) three sources: (1) imperfect knowledge of the system, (2) natural variability, and (3) anthropogenic emissions (Hallegate et al., 2012; Hawkins & Sutton, 2009). Multiple climate models are used to address the effects of simplifications in the climate system (Alfieri et al., 2018; McSweeney et al., 2012; Wilcke & Bärring, 2016) and multiple representative concentration pathways (RCPs) can cover the uncertainty regarding the extent of anthropogenic emissions (Van Vuuren et al., 2011).

Natural variability within the climate is an often-neglected source of uncertainty when analyzing flow extremes (Van der Wiel et al., 2019; Ward et al., 2010). Especially in international flood risk assessments, for example conducted in the framework of consultancy projects or other applied assessments, the derivation of future hazards is often based on a single or limited number of realizations from a number of GCMs. The use of single realizations does not reflect the full natural variability and may even project changes that are inconsistent with the climate change scenarios and may over or underestimate flood extremes. This can lead to erroneous definitions of adaptation pathways possibly demanding unnecessary expensive reinforcement programs (Haasnoot et al., 2013). Moreover, in general, the control climate (a historical period of 30 years) is too short to provide a realistic representation of extreme flood events.

There are two main causes of insufficient representation of natural variability and trends in the climate change impact assessment. First, the atmosphere is a very nonlinear system and the numerical solutions of climate models are highly sensitive to small perturbations under initial conditions (Aalbers et al., 2018; Deser et al., 2020; Zhu et al., 2019). According to Giorgi and Bi (2000), initial conditions influence the day-to-day occurrence as well as the frequency of occurrence of heavy precipitation events. Due to the chaotic nature of the climate models, each realization can lead to a different future, possibly even with opposite directions of change (Kew et al., 2011; Lutz et al., 2016). Second, the GCM simulation lengths for the control climate are too short to provide realistic estimates of extreme flood events such as the one in 100 years flood that is frequently used in flood risk vulnerability assessment and adaptation studies. By using multiple realizations from a single climate model, the data available for the extreme value analysis increase with the increasing number of realizations considered (Sterl et al., 2009; Van den Hurk et al., 2015).

Several studies exist where the use of perturbed ensembles of multiple-realizations has successfully been applied to overcome these shortcomings. For example, a perturbed ensemble approach was followed in the UK for the definition of the national climate scenarios considering multiple realizations of multiple climate models (Evans et al., 2004; Kay et al., 2020; Sayers et al., 2020; Warren et al., 2016). Probabilistic projections of changes in future river flows, means, and extremes were derived from a large set of perturbed parameter ensemble simulations for a set of RCPs (Murphy et al., 2020). This represents a best-practice that is not yet common in flood risk assessments worldwide.

This study does not aim to derive the best possible climate projections, it rather evaluates whether indeed more robust climate responses are obtained when multi realizations of a GCM-RCP combination are used. Hereto, we use 16 realizations from a single GCM (EC-EARTH; Hazeleger & Bintanja, 2012) for RCP8.5 to derive changes in future river flow. By using a single GCM-RCP combination, the ensemble uncertainty is isolated from other uncertainties. This enables the investigation of the variance among ensemble members and provides improved insights in (change in) natural variability presented by the GCM. For illustrative purposes, we estimate future changes in flow extremes for three locations along the river Rhine. The Rhine was chosen as an exemplary basin, as quite advanced climate impact assessments have been conducted for the Rhine basin (Görgen et al., 2010; Sperna Weiland et al., 2015; Te Linde et al., 2011). The basin can therefore be considered as a field laboratory with a large amount of data available, which allows for evaluation of the outcomes of the analysis.

## 2 | DATA AND METHODS

### 2.1 | River Rhine

The Rhine is one of the largest river basins in Western Europe and is intensively used for agriculture, industry, and navigation (Kwadijk & Rotmans, 1995; Van Alphen, 2016). The basin area is 185,000 $km^2$ with 58 million inhabitants of which more than 10 million live in flood-prone areas (ICPR, 2001; Khanal et al., 2019). The river originates in the Swiss Alps and flows along the Southern boundary between France and Germany and continues through Germany before it enters the Netherlands at Lobith (Te Linde et al., 2011; van Osnabrugge et al., 2017; Figure 1). On its course downstream, its regime changes from snowmelt to a combined rain-snowmelt-driven regime. At Lobith the average discharge is ~2200 $m^3 s^{-1}$. The maximum measured discharge of 12,600 $m^3 s^{-1}$ was observed in 1926 (Pinter

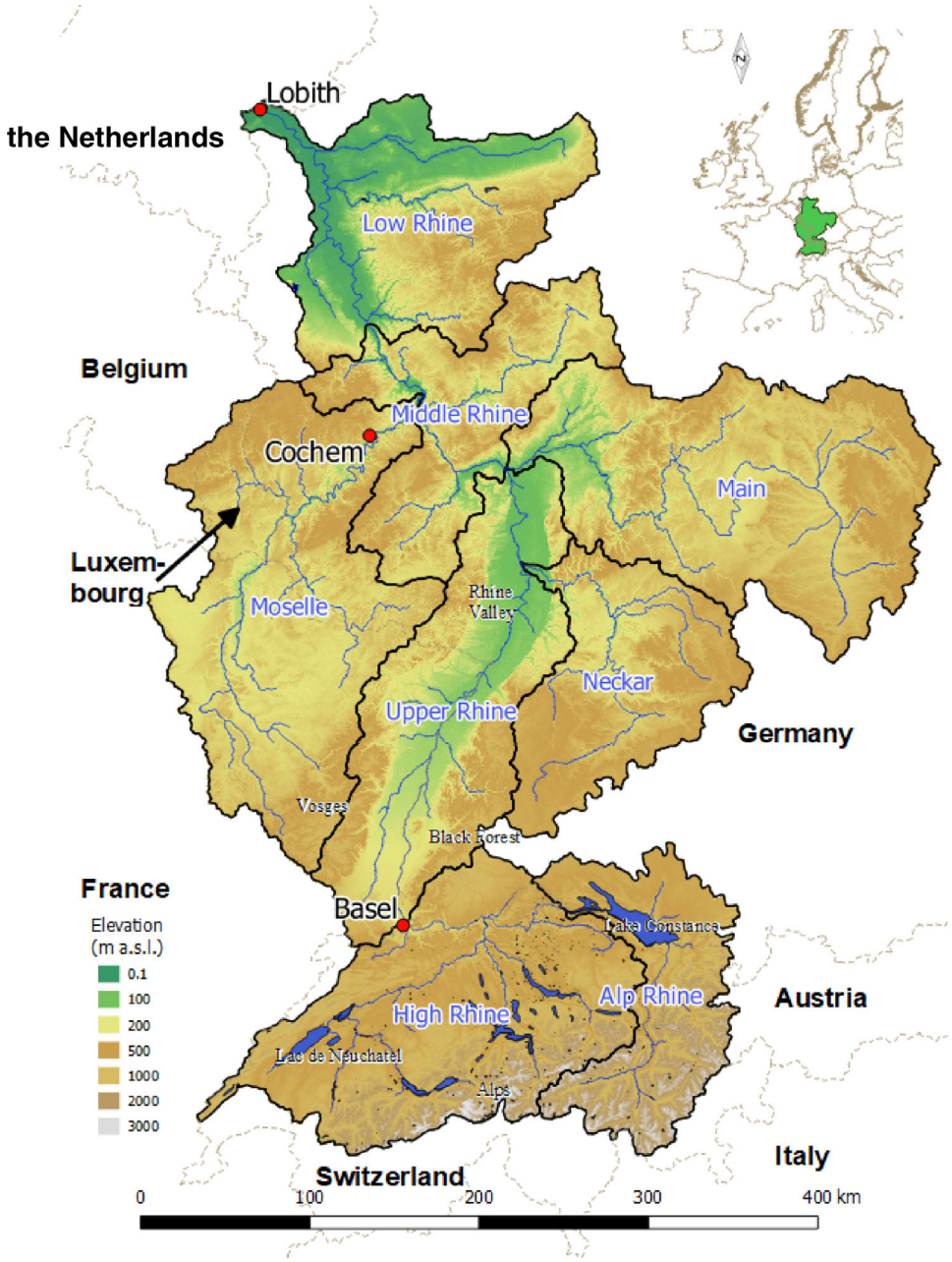


**FIGURE 1** Overview of the Rhine basin with the digital elevation model as background. The thick black lines delineate the eight major subcatchments with names in italic blue. The red dots show the locations of the three streamflow measurement stations used in the analysis. *Source*: van Osnabrugge et al. (2017)

et al., 2006). The major dikes along the Dutch part of the Rhine have been designed with safety levels varying between 1/1250 and 1/10,000 years (Kind, 2014).

## 2.2 | Historical datasets

### 2.2.1 | Discharge data

The analysis focuses on the simulated discharge extremes at three locations in the Rhine basin: Lobith, Basel, and Cochem (Table 1). The estimated extreme discharges at the station Lobith are used for the Dutch flood risk assessments and definition of the flood risk management plans. Basel and Cochem are included to analyze changes both in a snow-dominated and a rain-dominated sub-basin. The historical reference data were obtained from the Dutch National Water Authority (Rijkswaterstaat).

**TABLE 1** Stations considered in analysis (see locations in Figure 1)

| Station | Country | Present day regime type |
|---|---|---|
| Basel | Zwitserland | Snow-dominated |
| Cochem | Germany | Rain-dominated |
| Lobith | the Netherlands | Mixed |

#### 2.2.2 | Meteorological data

For hydrological model development and evaluation, the historical river discharges at these stations have also been simulated with the hydrological model used for the climate simulations. Hereto historical gridded time-series of precipitation from the station-based genRE dataset were used (Van Osnabrugge et al., 2017) together with station-based temperature and evaporation grids, the latter were calculated using the Makkink equation (Van Osnabrugge et al., 2018). The dataset has a spatial resolution of 1.2 × 1.2 km, an hourly time-step and covers the period 1998 to 2015.

### 2.3 | EC-Earth

EC-Earth is a GCM that uses the weather forecast model of the European Centre of Medium Range Weather Forecast (ECMWF) in its seasonal prediction configuration as a base (Hazeleger & Bintanja, 2012). The EC-Earth system model describes the global climate system and its evolution in time by a combination of coupled physical and biogeochemical processes. The integrated forecast system of the ECMWF forms the atmospheric component. The ocean component is based on the Nucleus for European Modelling of the Ocean. This analysis is based on data from EC-Earth version 2.3, that is the model version applied for the fifth phase of the Coupled Model Intercomparison Project (CMIP5).

A 16-member ensemble of GCM realizations from the EC-Earth climate model has been used. Each realization started-off with slightly different initial conditions that were obtained by small statistical perturbations of the model variables. Due to those small differences in each realization, the individual model realizations evolve differently. However, all realizations represent the same climatological conditions, so each realization represents a possibility how the climate could develop. This ensemble is used to assess the full range of natural climate variability and to obtain good statistics for extreme cases (Sterl et al., 2009). To ensure the change signal is as pronounced as possible, this analysis uses data for the most extreme pathway, RCP8.5.

We chose not to apply a bias-correction, downscaling, or a delta change approach to the EC-Earth data as these techniques can disturb the change signal (Cloke et al., 2013; Hagemann et al., 2011; Themeßl et al., 2012). Consequently, the presented absolute discharge values and the distributions derived from the raw simulated discharge values may be biased.

### 2.4 | Hydrological modeling

The hydrological model employed in this study is the wflow_sbm model (Imhoff et al., 2020; Schellekens et al., 2021). This is a distributed hydrological model with a regular grid of 1.2 × 1.2 km which runs on a daily time-step. The model structure consists of three main routines: (i) rainfall interception (after Gash, 1979), (ii) soil processes, and (iii) river drainage and overland flow. Precipitation entering each model cell is partly stored in the canopy as interception storage and depending on the temperature as snow. The remaining liquid water infiltrates into the soil. Water is taken from the soil and canopy through evapotranspiration. The water exchange in the soil is schematized with two vertical soil layers, the unsaturated zone and the saturated zone. Total runoff is the sum of the direct runoff, and the melt water that does not infiltrate into the soil and the baseflow (lateral subsurface flow from the saturated zone). This total runoff is routed along the river network as discharge with kinematic wave routing. Instead of model calibration we here use the model parameterization method of Imhoff et al. (2020)) specifically tested for the Rhine Basin. The method is based on vegetation and soil properties and is thus relatively independent of the model forcing data used and therefore most suitable for simulations with multiple climate models (Sperna Weiland et al., 2012). Continuous hydrological simulations were conducted with the gridded precipitation, temperature and Hargreaves potential evaporation daily data from the EC-Earth model for the period 1951 to 2100 as input.

### 2.5 | Statistical analysis for future flood risk assessment

For the statistical analysis the data was divided in four time-slices of 30 years, as shown in Table 2. A length of 30 years as control climate is recommended by the WMO; it is long enough to filter out any interannual variation or anomalies, yet short enough to not be influenced by a strong trend (WMO, 2017). For extreme value analysis, it is a very limited period often including only a small

**TABLE 2** Historical and future time horizons considered

| Time horizon | Years | Representative for the year |
|---|---|---|
| Far past | 1951–1980 | 1965 |
| Recent past | 1981–2010 | 1995 |
| Near future | 2036–2065 | 2050 |
| Far future | 2071–2100 | 2085 |

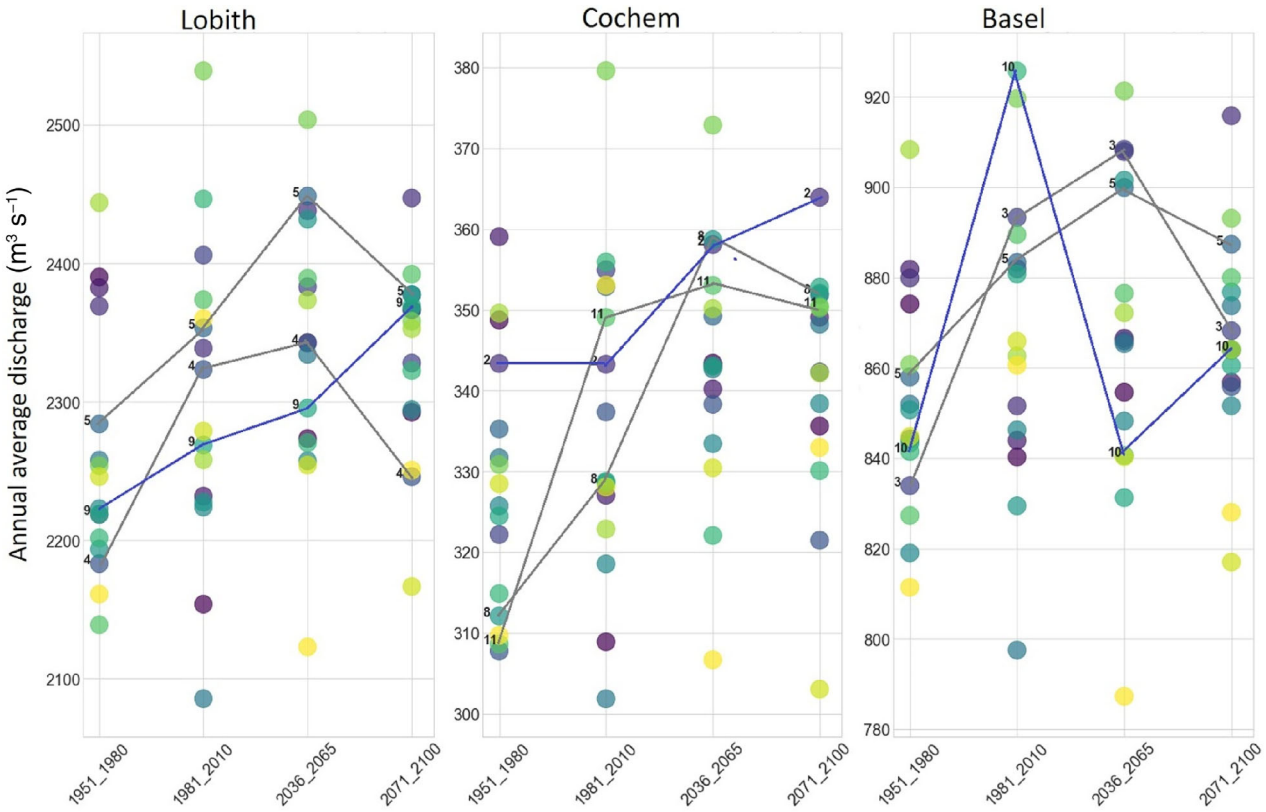


**FIGURE 2** Annual average discharge ($m^3\ s^{-1}$) plotted for the individual EC-Earth ensemble members for the historical periods and the near and far future. Each color represents the results of one of the ensemble members, color coding for the individual members is similar for all periods. Graphs provide (from left to right) results for Lobith, Cochem, and Basel, thus from downstream to upstream the river Rhine

number of (random) extremes. This makes the extreme value distribution highly uncertain and therefore this study does not go beyond return periods of 100 years. In the results section we will discuss that the use of the ensemble datasets will provide additional extremes that can be included in the statistical analysis following the approach of Van den Hurk et al. (2015) and Sterl et al. (2009).

The analysis of projected future changes focuses on two discharge statistics:

1. 30-year mean annual average discharge; and
2. extreme discharge for an occurrence frequency of once every 100 years.

The latter corresponds to a discharge or flood event that could potentially occur once every hundred years.

The extreme discharges are derived using the Gumbel distribution applied on annual maxima. A Gumbel distribution was chosen because the shape parameter is for all three locations close to zero.

## 3 | RESULTS

### 3.1 | Variation in projected changes from the set of initial conditions

To assess the influence of the selection of a single GCM-RCP realization, the projected changes have been assessed for each realization individually. Figure 2 presents the 30-year mean annual average discharge for all ensemble members for all time horizons of interest. The projected direction of change varies between the ensemble members. For example, for the flow Lobith, ensemble members 4 and 5 (light gray line) show an increase for 2050, and a decrease for 2100, that is, a hilly plot representing behavior that was not expected. Member 9 shows a continuous increase. For Cochem and Basel, we find similar variations between ensemble members. Selecting only one ensemble member results in very different projected discharge changes with respect to the historical periods. The projected increases could indicate a need for dike reinforcements, while the decreases indicate that the current protection levels are already

sufficient. Using only one of the realizations could thus possibly result in investments for adaptation measures that may not be needed.

Our results suggest that in light of the large variation between the ensemble members, the full set, or at least a set of ensemble members needs to be used for a reliable assessment of directions of change in average and extreme discharges (Figure 2). Therefore, we have combined the information from 16 ensemble members for each time horizon of 30 years (see Figure 3). The boxplots in Figure 3 present the distribution of the annual averages for the ensemble for all four time horizons.

For Lobith, the median discharge increases with time, leading to the highest median discharge by the end of the century. Annual mean discharge derived from the 30-year time-slice of the far past compared to the recent past is also lower. If we consider the ensemble uncertainty and focus on the boxes which represent the middle 50% of the ensemble projections, we see that in 2050, the uncertainty will likely be larger and the annual mean discharge can be higher than that in 2100. This hillyplot is similar to the behavior found for projections from single ensemble members; however, with the results grouped in single boxplots per time horizon, the overall variation decreases.

The results for Cochem are similar to Lobith although the variation in discharges projected by 2050 is smaller. The uncertainty in projected annual mean discharges at Lobith is a combination of the uncertainties in discharge projected for the upstream gages at Basel and Cochem. The intra-ensemble variation at Basel is much larger for 2050 than that for 2100, a similar result was found by Gobiet et al. (2013). The Alpine region is located in a transition zone, which is characterized by large uncertainties of the projected precipitation changes and thus Alpine river discharges (Heinrich et al., 2013). In general, the Europe climate change projections show a north–south pattern with reduced precipitation in Southern Europe in summer and increased precipitation in Northern Europe in winter. The transition zone is shifting northwards in summer and southwards in winter, the European Climate change oscillation (ECO; Giorgi & Coppola, 2007), and this is realized differently by the individual ensemble members.

For discharges with a return period of 100 years (RP100; Figure 4), the changes are more pronounced than the changes in annual mean discharge presented in Figure 3. For Lobith, more than 50% of the estimated discharge extremes for the near and far future are outside of

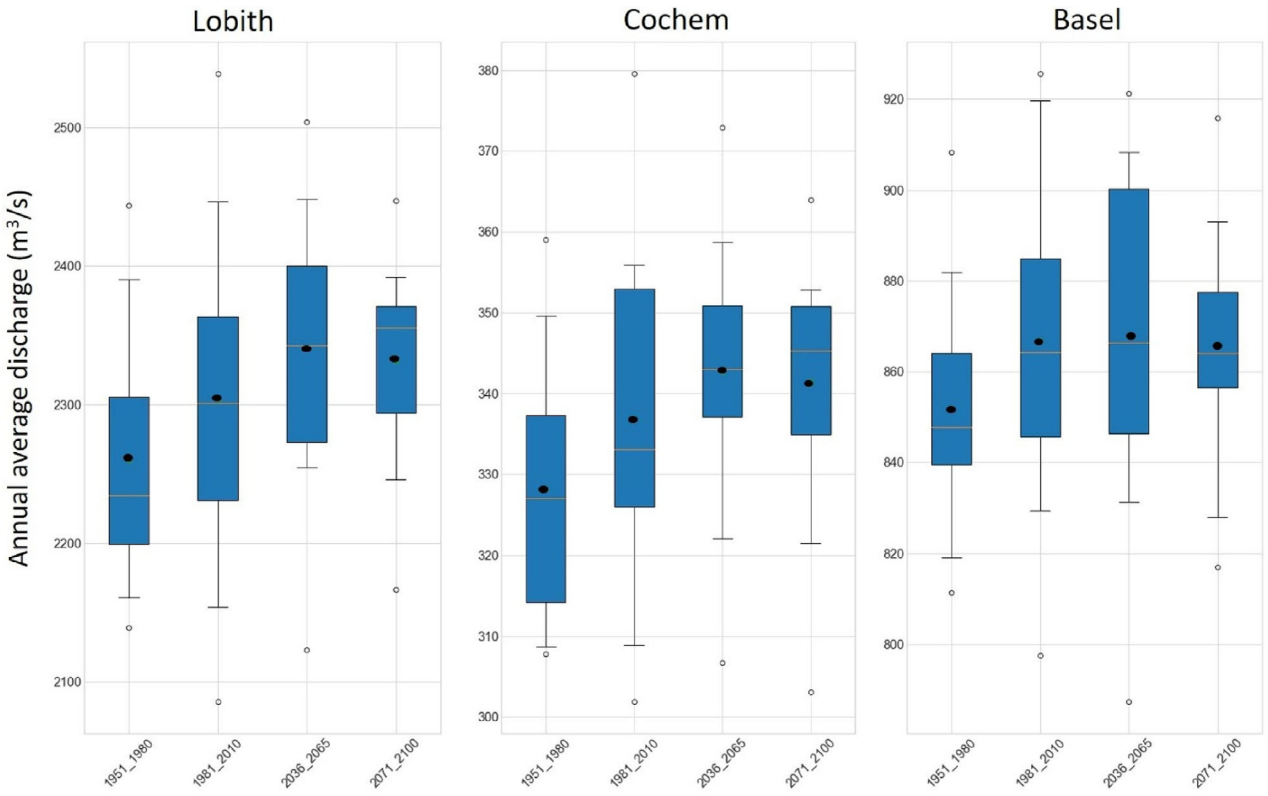


**FIGURE 3** Boxplots with the 30-year mean annual average discharge ($m^3\ s^{-1}$) derived from the full set of ensemble members for from left to right Lobith, Cochem, and Basel. The boxes represent the middle 50% range of annual averages, the whiskers represent the 95% range, and the outliers are presented by dots. The boxes contain the mean (black dot) and median (horizontal line)

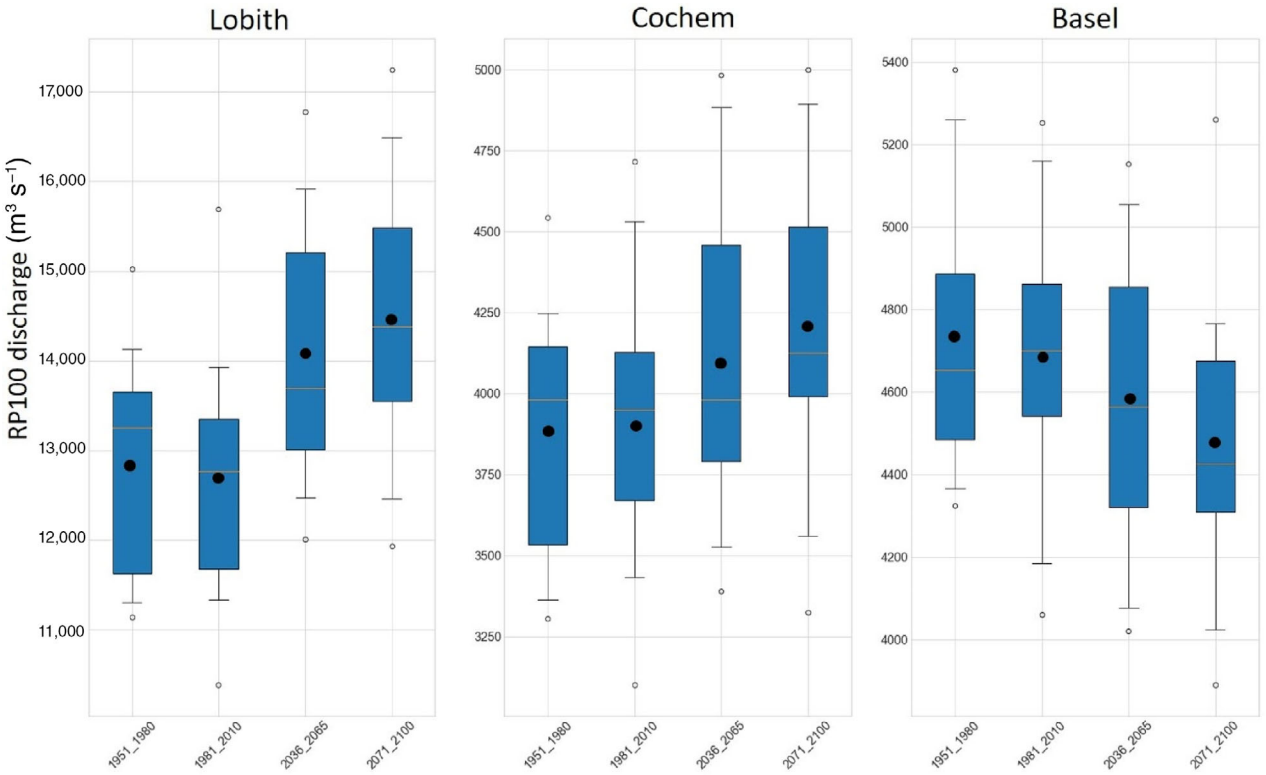


**FIGURE 4** Boxplots with the 30-year discharge extremes ($m^3\ s^{-1}$) estimated for a return period of 100 years (RP100) derived from the full set of ensemble members for from left to right Lobith, Cochem, and Basel. Layout similar to Figure 3

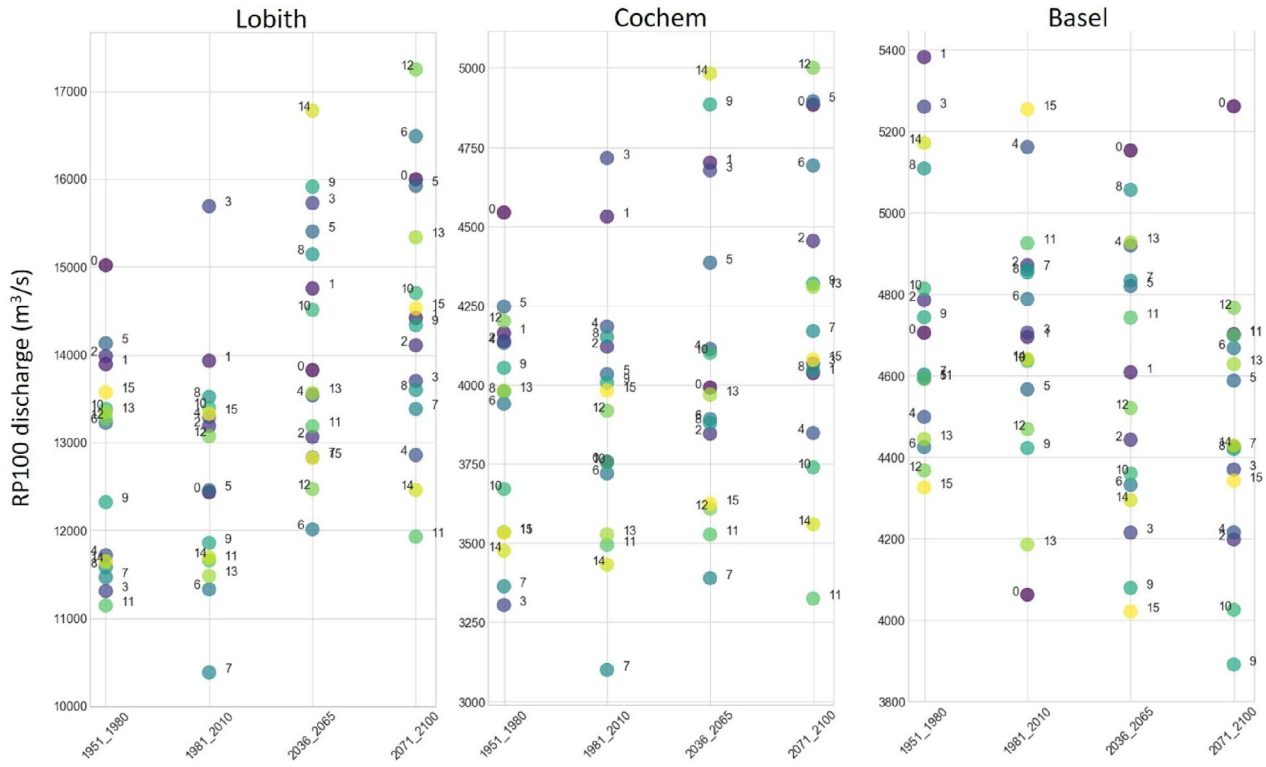


**FIGURE 5** Discharges ($m^3\ s^{-1}$) estimated for a return period of 100 years for the individual EC-Earth ensemble members for the historical periods and the near and far future. Each color and number represents the results of one of the ensemble members, color coding for the individual members is similar for all periods. Graphs provide (from left to right) results for Lobith, Cochem, and Basel

the range covered by the boxes for the recent and far past, representing the historical climate variability. This indicates that it is very likely that in the future discharges with a return period of 100 years will increase. By 2100, the RP100 discharge is projected to be higher than that in 2050. For Cochem, a similar change pattern can be found although less pronounced by 2050. For Basel, a likely decrease in extreme flood events that is outside the range of the current climate variability, is projected.

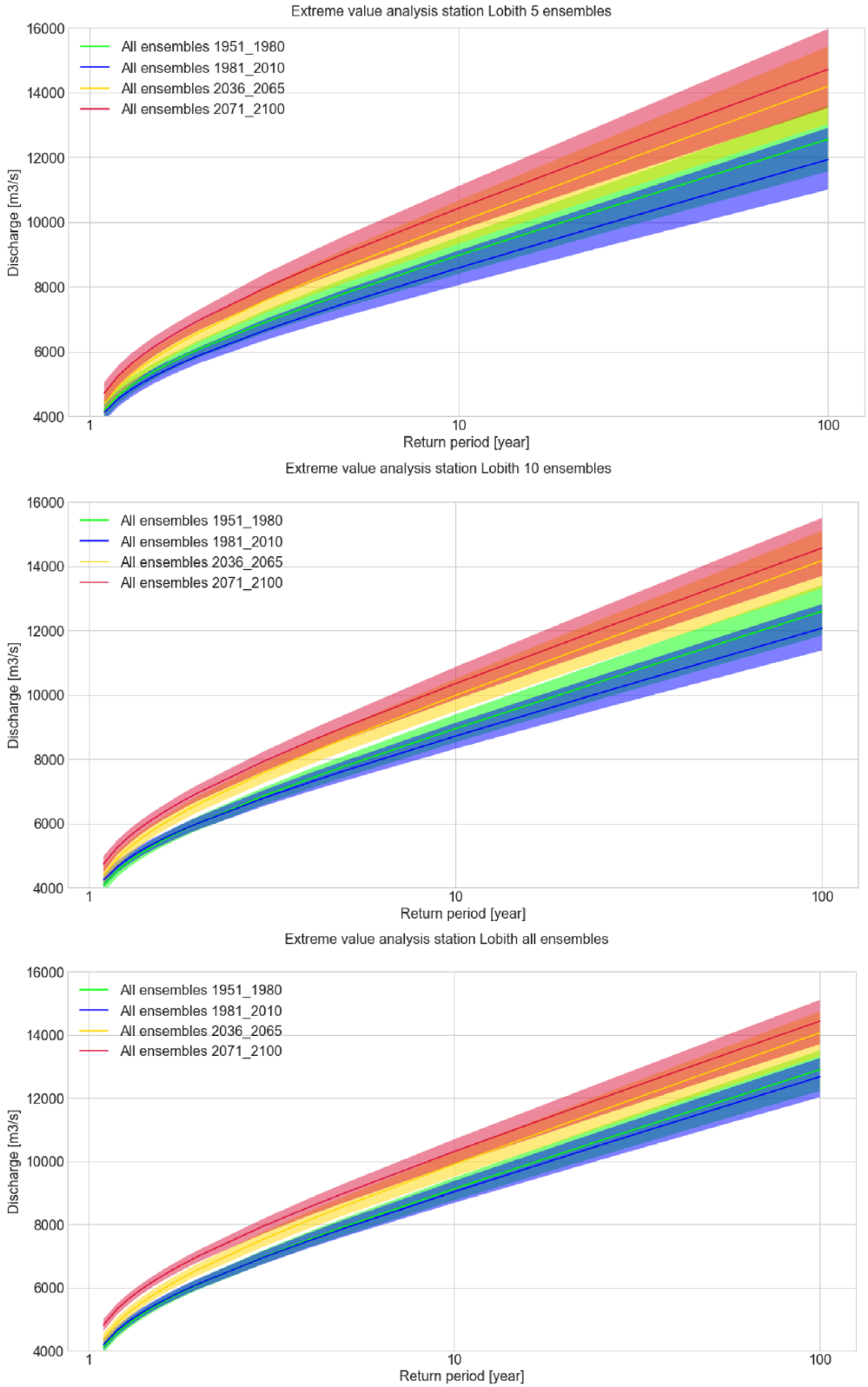


**FIGURE 6** Decrease in uncertainty bands of the estimated discharges ($m^3\ s^{-1}$) for Lobith for different time frames using the set of annual maxima for the 30-year time-slices of for (from top to bottom) 5, 10, and 16 ensemble members

To evaluate the variation in projected discharge change of extremes by individual ensemble members, Figure 5 has been included. Here, the discharge extremes refer to discharges occurring with a return period of 100 years. The change in RP100 is more pronounced; however, there is still a large overall bandwidth when the individual members are compared. The absolute values of discharge projected for 2100 show large variation for all three gage locations, for Lobith ranging from 12,000 to 17,000. And, although the projected discharge may be more alike after bias-correction, this confirms our hypothesis that a single realization cannot project whether protection against flood protection should be enhanced.

## 3.2 | The added value of using multirealizations

The additional benefit of using an ensemble set of projections is the increase of the number of available annual maxima that can be used to derive the extreme value distributions (Sterl et al., 2009; van den Hurk et al., 2015). This is achieved by pooling the annual maxima from the single time-series from the set of realizations all together in the statistical analysis. To assess the influence of the number of ensembles considered and thus the number of annual maxima available for the extreme value analysis, Gumbel distributions have been plotted based on ensembles of 5 realizations (150 annual maxima), 10 realizations (300 annual maxima), and 16 realizations (480 annual maxima). In Figure 6, the number of ensembles considered increases from top to bottom. The width of the uncertainty bands clearly decreases with the number of realizations considered, that is the uncertainty resulting from an incomplete representation of the natural climate variability decreases when a larger set is used. This is confirmed by the example in Figure 7 that presents the projected discharges for RP100 (with corresponding uncertainty bands) for the period 2071–2100 obtained from an increasing number of realizations (x-axis). Expanding the number of ensemble member first stabilizes the mean return period (blue/black lines, Figure 7), with even more members also the bandwidth of the natural variability does not change any more (black/blue lines, Figure 7). This provides insight in the actual natural variability. In the example of this study, stabilization of the bandwidth of the natural variability seems to occur around 14 members. However, since there are only 16 members available it is unsure whether adding more ensemble members would further increase the robustness of the analysis.

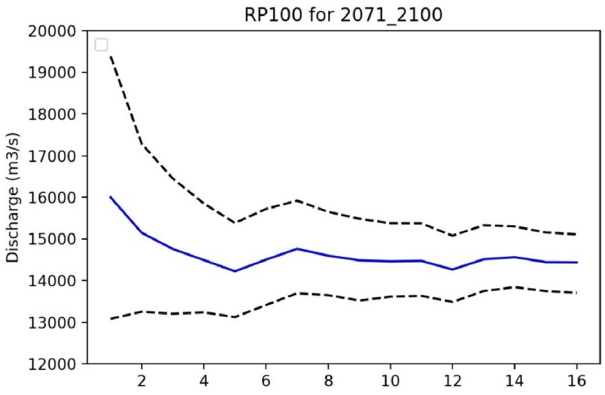


**FIGURE 7** Decreasing uncertainty ranges (bands displayed with dashed black) and converging RP100 values (blue) with increasing ensemble members derived with the Gumbel distribution

## 3.3 | Comparison with existing extreme value distributions for the Rhine

One of the most thorough and official Dutch assessment of climate change impacts on discharge extremes for the Rhine at Lobith is conducted for the KNMI'14 scenarios (KNMI, 2014; Sperna Weiland et al., 2015). The KNMI'14 scenarios are based on a large set of CMIP5 climate models with for some of them multiple realizations. The four KNMI'14 scenarios were constructed such that they represent changes according to RCP4.5, RCP6.0 and RCP8.5 obtained from this set of CMIP5 models.

Figure 8 presents the discharge extremes projected for Lobith for return periods of 100 and 10 years obtained in the KNMI'14 study and the current study. From the set of four KNMI'14 scenarios, the most extreme scenario was taken as it corresponds most with RCP8.5. This scenario exhibits the largest change in air circulations and the largest temperature increase. For RP100, the KNMI'14 scenarios are captured by the here projected discharge range. For RP10, the KNMI'14 scenarios projected higher discharge extremes over time than the EC-Earth projections. It is known that the KNMI'14 projected discharges for 2050 are relatively high (Sperna Weiland et al., 2014), taken this into account, it can be concluded that the resemblance between this study and the KNMI'14 scenarios is reasonable.

## 3.4 | Extreme discharge projections for Cochem and Basel

As discussed in the previous section, we used all members of the ensemble to perform the extreme value analyses to include the most robust information on natural

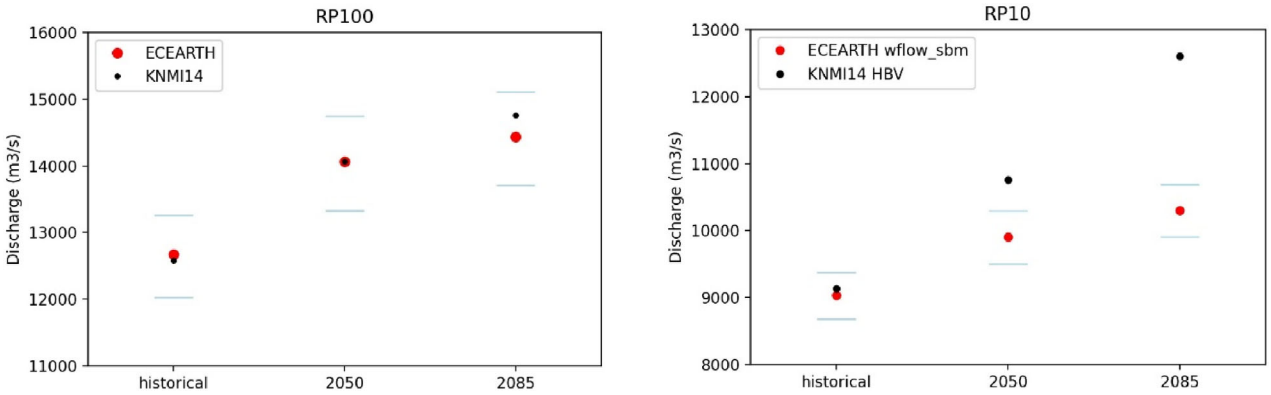


**FIGURE 8** Discharge extremes for RP100 (left) and RP10 (right) projected for the KNMI'14 scenarios (black) and the EC-Earth ensemble set (red, with light blue uncertainty bands)

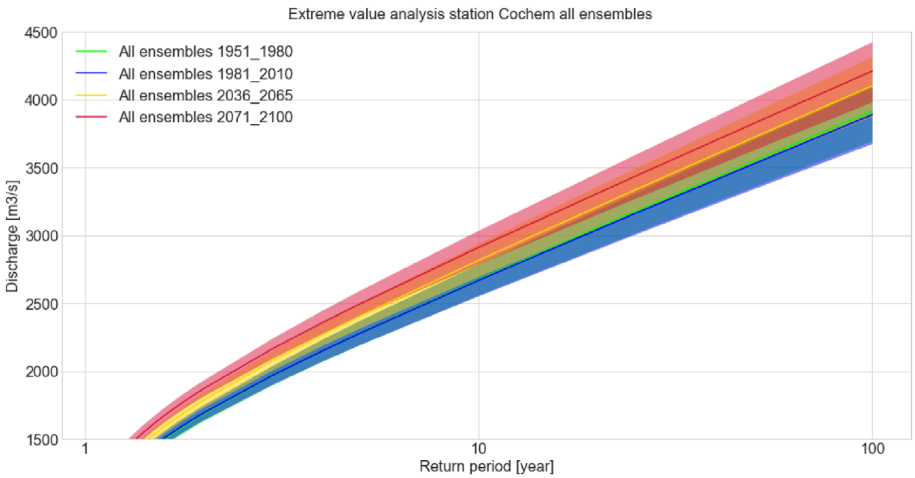


**FIGURE 9** Estimated discharges ($m^3\ s^{-1}$) for Cochem for different time frames using the set of annual maxima for the 30-year time-slices of 16 ensemble members

variability. Therefore, we have included Figure 9 for Cochem and Figure 10 for Basel with the Gumbel Distributions derived from the total of 480 annual maxima for all four time horizons. In this way, all available information has been incorporated in the final extreme value distributions. In line with the results presented in Figure 4 the Gumbel distributions indicate an increase in RP100 discharge for Lobith and Cochem but a decrease for Basel.

High flows at Cochem and Lobith occur mostly in winter or spring as a result of continuous precipitation over large parts of the upstream basin, sometimes (in combination with) snowmelt in Germany (see the regime plots in Figure 11). Yet, high flows at Basel occur often in summer time (Görgen et al., 2010; Figure 11) and are a result of the combination of snowmelt and heavy precipitation in the Alps. In the far future, due to temperature increases in the Alpine part of the basin, the regime at Basel will become a mixed snow and rainfall regime and snowmelt will contribute less to discharge peaks in early summer (Rottler et al., 2021). There will be less seasonal variation in flow and winter flow will reduce (see Figure 11). Another consequence of the Alpine regime shift is that the discharge peaks downstream at Lobith will likely occur earlier in the year. In the Moselle, with future increasing temperatures, snow accumulation will decrease and more rainfall will directly runoff in winter. This may lead to slight increases in winter flows at Cochem.

Next to these physical system changes, Figure 11 also provides information on the value of the set of realizations. For the historical period at Lobith and Basel, the consistency between the realizations is high. The signal is influenced by snowmelt caused by temperature rise during spring and summer. In the future, when the influence of snow becomes less important, the variability between the realizations for the timing of the highest flow month increases, especially for Lobith. This is caused by the uncertainty in precipitation projections, the large natural variability in precipitation, and the faster discharge response of rain water compared to melt water. This variation can only be captured by using the ensemble of realizations.

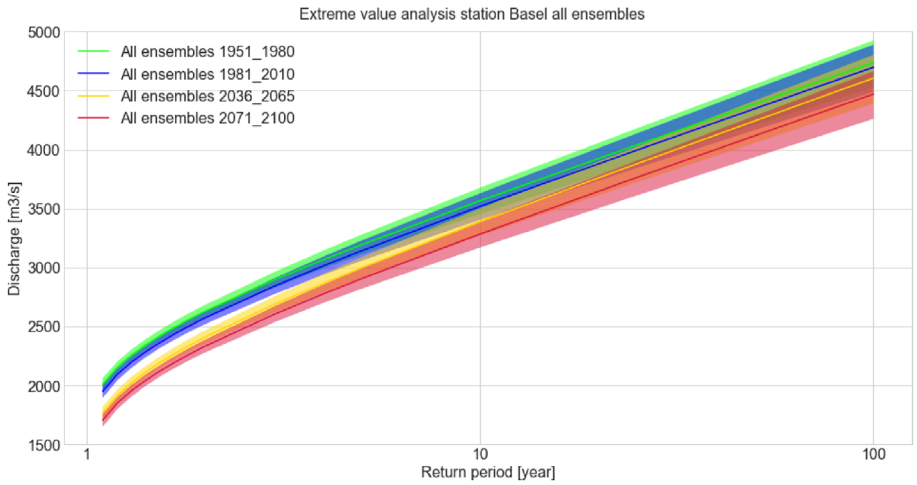


**FIGURE 10** Estimated discharges for Basel for different time frames using the set of annual maxima for the 30-year time-slices of 16 ensemble members

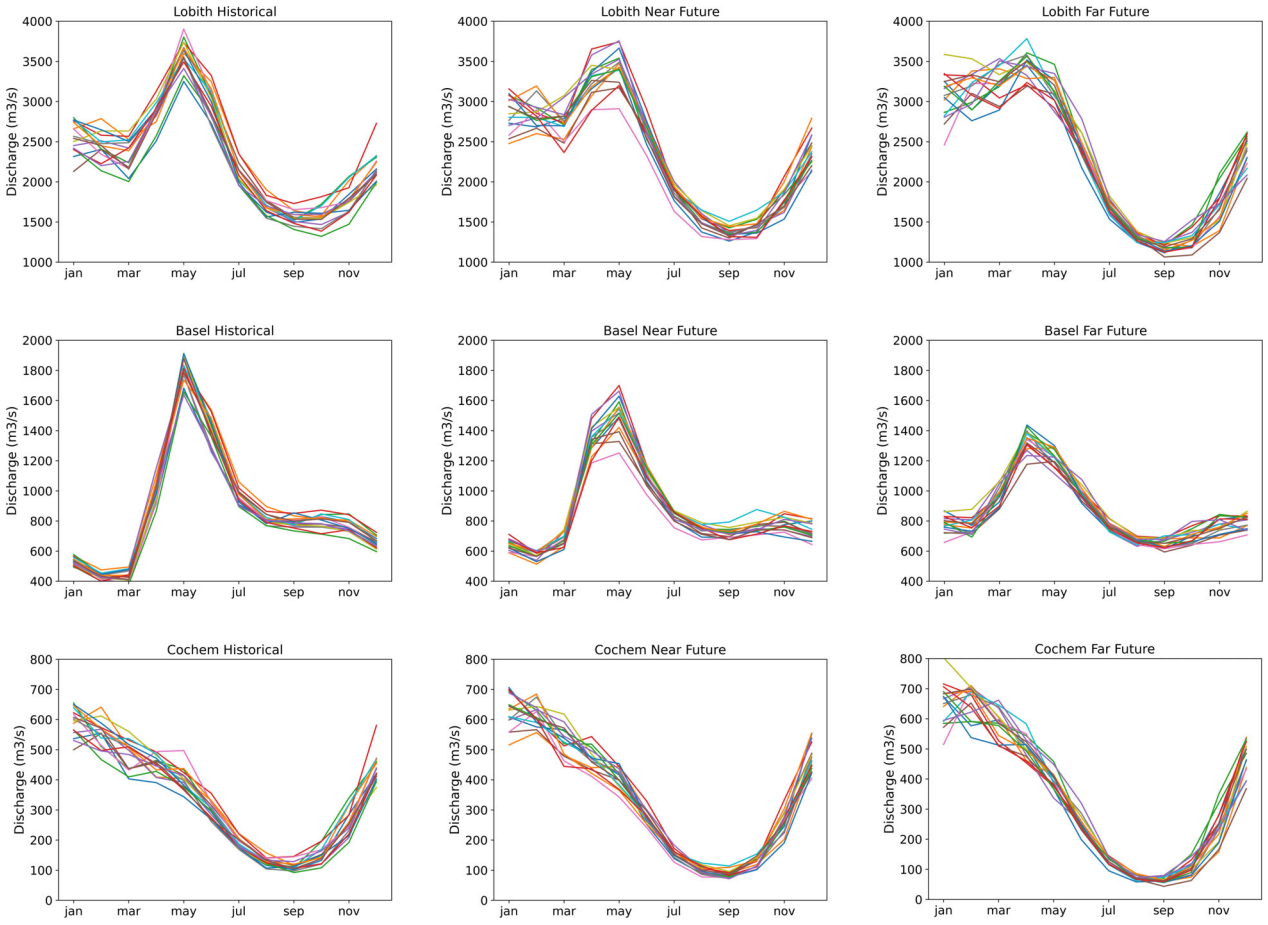


**FIGURE 11** Discharge regime plots for—from top to bottom—Lobith, Basel, and Cochem for—from left to right—the historical period (1981–2010), the near future (2036–2065) and the far future (2071–2100). Each colored line represents the regime calculated from the 30-year time-series of one realization

## 3.5 | Implications of the climate change projections along the Rhine

For both Lobith and Cochem, the 50% uncertainty band (between the 25 and 75 percentile values) obtained from the full ensemble projects a gradual increase in annual discharge for RCP8.5. For Basel, the range of projected changes is much wider by 2050 with overall higher annual average discharges than observed in the past. After 2050, for Basel, a small decrease in the median is projected. The increase projected for the first half and the decrease for the second half of the century can be a result of the glaciers that are melting and currently contribute to the discharges but may for a large share be gone by

2085 (Junghans et al., 2011), yet an exact quantification of this contribution would require an advanced glacier model (Stahl et al., 2017). Furthermore, projected temperature increases lead to less snow accumulation and earlier snowmelt reducing the snowmelt-driven peak discharge at Basel. Snowmelt-driven Alpine discharge peaks will likely occur earlier in the year as has already been observed (Görgen et al., 2010; Zampieri et al., 2015). Earlier Alpine flood peaks may coincide with the discharge peaks from the rainfed sub-basins downstream, like the Moselle, where the RP100 discharge is projected to increase. The difference between 2050 (RP100 increase) and 2100 (RP100 decrease) for Basel may as well be a result of the ECO (Giorgi & Coppola, 2007), the transition zone that moves over the Alps and will increase the uncertainty particularly for the near future.

For Lobith, the majority of the projected future annual average discharges (i.e., the 50% range) is already covered by the historical climate variability (the 95% range for the period 1951 to 1980). There will be little effect of the changes in annual average discharge on the Rhine. Yet, the results presented in Figure 4 indicate that increases of future discharges with a return period of 100 years are very likely for Cochem and Lobith. This confirms the need for an increase of the safety levels for the dikes along the Rhine (Sperna Weiland et al., 2015). In addition, discharges that currently correspond to a return period of 100 years will occur more frequent. As a consequence, the Rhine will be at higher water levels more often. This increases the duration and severity of the load on dikes and could lead to piping or even dike instability (Vorogushyn et al., 2009).

The here projected changes are in line with earlier studies investigating the impacts of climate change on the river Rhine (Görgen et al., 2010; Sperna Weiland et al., 2015; Te Linde et al., 2011; Zampieri et al., 2015).

## 4 | DISCUSSION

Projected changes in river flow extremes are shown to be highly dependent on the GCM realization selected for the assessment. This is consistent with earlier conclusions on the large internal variability in GCMs and RCMs represented by perturbed model ensembles (Aalbers et al., 2018; Kew et al., 2011; Rinke et al., 2004; van der Wiel et al., 2019; Zhu et al., 2019). Here, we demonstrated the large variation in projected river flow extremes, mean flow, and timing of the flow regime that exists between single realizations. As projected, increases in flow extremes will increase flood risk and require large investments in adaptation, and the reliability of the projected discharge extremes is extremely important.

Advanced climate impact assessments that consider an ensemble of perturbed realizations, multiple climate models and RCPs exist (Evans et al., 2004; Kay et al., 2020; Murphy et al., 2020; Sayers et al., 2020). Yet, these often involve important contributions from climate scientists and it is not common practice in flood risk assessment. Here, we contribute to existing scientific literature by showing the added value of using multiple realizations for flood risk assessment and by illustrating how individual realizations can have different outcomes on river flow projections.

The aim of the current study was to explore the potential consequences of limited GCM realizations on flood risk assessments, rather than providing an optimal set of projections. Extended assessments of future discharge changes in the Rhine exist (Görgen et al., 2010). For example, adaptation planning in the Netherlands relies on the discharge extremes projected for the Dutch KNMI'14 scenarios (Sperna Weiland et al., 2014) that involved evaluation of a large set of CMIP5 GCMs, a carefully constructed set of four representative RCM-based climate change scenarios and a weather generator for the derivation of synthetic rainfall time-series that were used in the flood modeling chain. The here projected RP100 discharges and their uncertainty ranges cover the RP100 discharges projected for the KNMI'14 scenarios well. This is less the case for the RP10 values. Still, the approach of combining annual maxima from multiple realizations in extreme values can also be promising for data-sparse basins.

The size of the ensemble was limited by the number of readily available EC-Earth simulations. Increasing the number of realizations from 5 to 16 reduced the uncertainty bands and both the projected absolute values and uncertainty bands seemed to converge. With an increased number of ensemble members, the uncertainty in projections could possibly further be reduced as the variation may not fully be captured by the 16 members yet. There will always remain a tradeoff between the need for the reduction of uncertainties and the required computational costs.

The climate model temperature and precipitation time-series have not been bias-corrected. This was elaborately done to avoid any disturbance of the climate change signals. According to Willkofer et al. (2018), who evaluated the influence of bias-correction methods on streamflow projections for Bavarian catchments in Germany, changes in high flows were poorly represented by any bias corrected model results. The approaches assessed failed to properly capture extreme value statistics. Other studies found similar results even with advanced bias-correction techniques (Cloke et al., 2013; Hagemann et al., 2011; Themeßl et al., 2012). To allow

for a transparent evaluation of the variation within the ensemble, we decided to avoid any disturbing influence and therefor did not apply a bias-correction. Furthermore, for the main message of the current paper bias-correction is not essential, without bias-correction we can more clearly demonstrate the variation. Still, the fact that no bias-correction was applied in this study implies that the absolute discharge values can be biased. In addition, the use of lower resolution GCM data and not RCM data will have resulted likely in even larger biases and the possible underestimation of precipitation extremes cannot be overcome with the set of realizations used here as they are all based on the same model structure.

The analysis is based on a single GCM to isolate the uncertainties introduced by perturbed ensemble members from the other sources of uncertainy (i.e., RCPs and GCMs). The assumption is made that this variation is in general present in any GCM. The ensemble members here follow a different realization of the climate under the same climatological forcing. However, since the same GCM is applied in all realizations, the model uncertainty is not addressed in this type of analysis (Hawkins & Sutton, 2009). The ensemble members used here cannot be considered to be fully independent (see also Ward et al., 2012), and it is yet to be confirmed by extending the analysis to other GCMs. In an ideal flood risk assessment multiple GCMs, RCMs, and ensemble members are considered.

This study addresses changes in the flow regime of the river Rhine as well. These changes are influenced by snow as well as glacier melt (Stahl et al., 2017). Within the wflow_sbm model version glaciers and snow are treated as a single compartment. We performed continuous model simulations from 1951 to 2100 and over time the volume of the snow pack decreases due to rising temperatures. This is only a simplified representation of the actual glacier retreat. In future work, the contribution of glacier melt to streamflow can better be represented using a separate glacier module where melt is treated differently from snow.

While this study follows a top-down analysis, starting from climate projections toward the estimate of extreme discharges in the future, the uncertainty of future changes is very high. An alternative approach is a bottom-up analysis (Shortridge & Zaitchik, 2018) which allows for a switch from a discussion on the probability of such changes to the effect on societal functioning. This consists, for example, of using existing measured data and gradually perturb it with different degrees of change while evaluating the system performance at all times. This allows for a good understanding of the degrees of change the system is able to cope with, see also the Decision Tree Framework (DTF) approach (Ray & Brown, 2015).

## 5 | CONCLUSIONS

Nowadays, future flood risk assessments often account for uncertainties in future anthropogenic emissions by considering multiple RCPs (Hempel et al., 2013; Sperna Weiland et al., 2015; Winsemius et al., 2013). The imperfect knowledge about, and representation of, the system is considered by using projections from multiple GCMs. Yet, uncertainty introduced by the incomplete representation of natural variability can be as important, especially when focusing on flood extremes. Still this is not always accounted for.

In the study, we explored the impact of the incomplete representation of natural variability in a flood risk assessment. To this end we forced wflow_sbm with 16 EC-Earth members and explored the differences between individual realizations and change in river flow under different return periods for a varying number of ensemble members. We conclude that for the Rhine, the assessment of future flow extremes highly depends on the selected GCM realization. Consequently, the selection of one realization can highly influence the outcome of a flood risk assessment and thus the resulting adaptation strategy and related investments. By increasing the number of realizations considered in the extreme value analysis, the future projections tend to converge, thus increasing the confidence in projected changes.

The differences between the historical and future flow regimes for Lobith and Basel demonstrated that when the cause of the changes is complex and originates from changes in uncertain snow and rainfall patterns, the ensemble information can also be very valuable.

The results of this study imply that flood risk assessments based on single GCM realizations should be treated with care and the use of multiple realizations should be adopted worldwide.

## ACKNOWLEDGMENT

The observed discharge data for Basel, Cochem, and Lobith were kindly provided by the Dutch National Water Authority (Rijkswaterstaat), the Netherlands. KNMI made the ensemble of EC-Earth datasets available for this study. The research was funded using the Deltares Strategic Research funding provided by the Dutch Government.

## DATA AVAILABILITY STATEMENT

Data available on request from the authors. The data that support the findings of this study are available from the corresponding author upon reasonable request.

## ORCID

*Frederiek Sperna Weiland* https://orcid.org/0000-0002-6033-979X

## REFERENCES

Aalbers, E., Lenderink, G., van Meijgaard, E., & van den Hurk, B. J. J. M. (2018). Local-scale changes in mean and heavy precipitation in Western Europe, climate change or internal variability? *Climate Dynamics*, *50*(11–12), 4745–4766. https://doi.org/10.1007/s00382-017-3901-9

Alfieri, L., Dottori, F., Betts, R., Salamon, P., & Feyen, L. (2018). Multi-model projections of river flood risk in Europe under global warming. *Climate*, *6*, 16. https://doi.org/10.3390/cli6010006

Cloke, H. L., Wetterhall, F., He, Y., Freer, J. E., & Pappenberger, F. (2013). Modelling climate impact on floods with ensemble climate projections. *Quarterly Journal of the Royal Meteorological Society*, *139*(671), 282–297.

DEFRA (2012). *The UK Climate Change Risk Assessment 2012 Evidence Report [online]*. http://www.defra.gov.uk/environment/climate/government/

Deser, C., Lehner, F., Rodgers, K. B., Ault, T., Delworth, T. L., DiNezio, P. N., Fiore, A., Frankignoul, C., Fyfe, J. C., Horton, D. E., Kay, J. E., Knutti, R., Lovenduski, N. S., Marotzke, J., McKinnon, K. A., Minobe, S., Randerson, J., Screen, J. A., Simpson, I. R., & Ting, M. (2020). Insights from Earth system model initial-condition large ensembles and future prospects. *Nature Climate Change*, *10*, 277–286. https://doi.org/10.1038/s41558-020-0731-2

Evans, E., Ashley, R., Hall, J., Penning-Rowsell, E., Saul, A., Sayers, P., Thorne, C., & Watkinson, A. (2004). *Foresight. Future flooding. Scientific summary: Volumes I and II*. Office of Science and Technology.

Felder, G., Gómez-Navarro, J. J., Zischg, A., Raible, C. C., Röthlisberger, V., Bozhinova, D., Martius, O., & Weingartner, R. (2018). From global circulation to local flood loss: Coupling models across the scales. *Science of the Total Environment*, *635*, 1225–1239. https://doi.org/10.1016/j.scitotenv.2018.04.170

Forzieri, G., Feyen, L., Russo, S., Vousdoukas, M., Alfieri, L., Outten, S., Migliavacca, M., Bianchi, A., Rojas, R., & Cid, A. (2016). Multi-hazard assessment in Europe under climate change. *Climatic Change*, *137*, 105–119. https://doi.org/10.1007/s10584-016-1661-x

Gash, J. H. C. (1979). An analytical model of rainfall interception by forests. *Quarterly Journal of the Royal Meteorological Society*, *105*, 43–55.

Giorgi, F., & Bi, X. (2000). A study of internal variability of a regional climate model. *Journal of Geophysical Research*, *105*(D24), 29503–29521. https://doi.org/10.1029/2000JD900269

Giorgi, F., & Coppola, E. (2007). European climate-change oscillation (ECO). *Geophysical Research Letters*, *34*(2007), L21703.

Gobiet, A., Kotlarski, S., Beniston, M., Heinrich, G., Rajczak, J., & Stoffel, M. (2013). 21st century climate change in the European Alps: A review. *Science of the Total Environment*, *493*, 1138–1151. https://doi.org/10.1016/j.scitotenv.2013.07.050

Görgen, K., Beersma, J., Brahmer, G., Buiteveld, H., Carambia, M., de Keizer, O., Krahe, P., Nilson, E., Lammersen, R., Perrin, C. & Volken, D. (2010). *Assessment of climate change impacts on discharge in the Rhine River basin: Results of the RheinBlick2050 project*. (CHR report, I-23), 229 pp., ISBN 978-90-70980-35-1.

Hallegatte, S., Shah, A., Lempert, R., Brown, C., & Gill, S. (2012). Investment decision making under deep uncertainty: application to climate change. Policy Research Working Paper; No. 6193. World Bank, Washington, DC. © World Bank. https://openknowledge.worldbank.org/handle/10986/12028 License: CC BY 3.0 IGO.

Haasnoot, M., Kwakkel, J. H., Walker, W. E., & ter Maat, J. (2013). Dynamic adaptive policy pathways: A method for crafting robust decisions for a deeply uncertain world. *Global Environmental Change*, *23*(2), 485–498. https://doi.org/10.1016/j.gloenvcha.2012.12.006

Hagemann, S., Chen, C., Haerter, J. O., Heinke, J., Gerten, D., & Piani, C. (2011). Impact of a statistical bias correction on the projected hydrological changes obtained from three GCMs and two hydrology models. *Journal of Hydrometeorology*, *12*(4), 556–578.

Hawkins, E., & Sutton, R. (2009). The potential to narrow uncertainty in regional climate predictions. *Bulletin of the American Meteorological Society*, *90*(8), 1095–1107. https://doi.org/10.1175/2009BAMS2607.1

Hazeleger, W., & Bintanja, R. (2012). Studies with the EC-Earth seamless Earth system prediction model. *Climate Dynamics*, *39*(11), 2609–2610. https://doi.org/10.1007/s00382-012-1577-8

Heinrich, G., Gobiet, A., Truhetz, H. & Mendlik, T (2013) *Expected climate change and its uncertainty in the Alpine region: Extended uncertainty assessment of the reclip: Century and ENSEMBLES multi-model dataset* (Wegener Center Scientific Report) 50.

Hempel, S., Frieler, K., Warszawski, L., Schewe, J., & Piontek, F. (2013). A trend-preserving bias correction—The ISI-MIP approach. *Earth System Dynamics*, *4*(2), 219–236. https://doi.org/10.5194/esd-4-219-2013

ICPR. (2001). *Atlas of flood danger and potential damage due to extreme floods of the Rhine [online]*. International Commission on the Protection of the Rhine. http://www.iksr.org/

Imhoff, R. O., van Verseveld, W. J., van Osnabrugge, B., & Weerts, A. H. (2020). Scaling point-scale (pedo)transfer functions to seamless large-domain parameter estimates for high-resolution distributed hydrologic modeling: An example for the Rhine River. *Water Resources Research*, *56*, e2019WR026807. https://doi.org/10.1029/2019WR026807

IPCC (2014). R. K. Pachauri & L. A. Meyer, *Climate Change 2014: Synthesis Report. Contribution of Working Groups I, II and III to the Fifth Assessment Report of the Intergovernmental Panel on Climate Change*, (151). Geneva, Switzerland: IPCC.

Junghans, N., Cullmann, J., & Huss, M. (2011). Evaluating the effect of snow and ice melt in an alpine headwater catchment and further downstream in the river Rhine. *Hydrological Sciences Journal*, *56*, 981–993. https://doi.org/10.1080/02626667.2011.595372

Kay, A. L., Watts, G., Wells, S. C., & Stuart, A. (2020). The impact of climate change on U.K. river flows: A preliminary comparison of two generations of probabilistic climate projections. *Hydrological Processes*, *34*(4), 1081–1088. https://doi.org/10.1002/hyp.13644

Kew, S. F., Selten, F. M., Lenderink, G., & Hazeleger, W. (2011). Robust assessment of future changes in extreme precipitation over the Rhine basin using a GCM. *Hydrology and Earth System Sciences*, *15*, 1157–1166. https://doi.org/10.5194/hess-15-1157-2011

Khanal, S., Lutz, A. F., Immerzeel, W. W., Vries, de, H. d., Wanders, N., & Hurk, B. v. d. (2019). The impact of meteorological and hydrological memory on compound peak flows in the Rhine river basin. *Atmosphere*, *10*(4), 171. https://doi.org/10.3390/atmos10040171

Kind, J. (2014). Efficient flood protection standards for The Netherlands. *Journal of Flood Risk Management*, *7*, 103–117. https://doi.org/10.1111/jfr3.12026

KNMI (2014) *KNMI'14: Climate change scenarios for the 21st Century—A Netherlands perspective* (Scientific Report WR2014-01) Bart van den Hurk, Peter Siegmund, Albert Klein Tank, Jisk Attema, Alexander Bakker, Jules Beersma, Janette Bessembinder, Reinout Boers, Theo Brandsma, Henk van den Brink, Sybren Drijfhout, Henk Eskes, Rein Haarsma, Wilco Hazeleger, Rudmer Jilderda, Caroline Katsman, Geert Lenderink, Jessica Loriaux, Erik van Meijgaard, Twan van Noije, Geert Jan van Oldenborgh, Frank Selten, Pier Siebesma, Andreas Sterl, Hylke de Vries, Michiel van Weele, Renske de Winter and Gerd-Jan van Zadelhoff. (Eds.) KNMI. www.climatescenarios.nl

Kwadijk, J. C. J., & Rotmans, J. (1995). The impact of climate change on the river Rhine: A scenario study. *Climatic Change*, *30*(4), 397–425.

Lutz, A. F., ter Maat, H. W., Biemans, H., Shrestha, A. B., Wester, P., & Immerzeel, W. W. (2016). Selecting representative climate models for climate change impact studies: An advanced envelope-based selection approach. *International Journal of Climatology*, *36*, 3988–4005. https://doi.org/10.1002/joc.4608

McSweeney, C. F., Jones, R. G., & Booth, B. B. (2012). Selecting ensemble members to provide regional climate change information. *Journal of Climate*, *25*, 7100–7121. https://doi.org/10.1175/JCLI-D-11-00526.1

Murphy, J.M., Brown, S. and Harris, G (2020) UKCP Additional Land Products: Probabilistic Projections of Climate Extremes, Met Office. Available from https://www.metoffice.gov.uk/binaries/content/assets/metofficegovuk/pdf/research/ukcp/ukcpprobabilistic-extremes-report.pdf

Pinter, N., Van der Ploeg, R. R., Schweigert, P., & Hoefer, G. (2006). Flood magnification on the river Rhine. *Hydrological Processes*, *20*, 147–164.

Ray, P. A., & Brown, C. M. (2015). *Confronting climate uncertainty in water resources planning and project design: The decision tree framework*. World Bank. License: Creative Commons Attribution CC BY 3.0 IGO. https://doi.org/10.1596/978-1-4648-0477-9

Rinke, A., Marbaix, P., & Dethloff, K. (2004). Internal variability in Arctic regional climate simulations: Case study for the SHEBA year. *Climate Research*, *27*(3), 197–209.

Rottler, E., Bronstert, A., Bürger, G., & Rakovec, O. (2021). Projected changes in Rhine river flood seasonality under global warming. *Hydrology and Earth System Sciences*. *25*, 2353–2371. https://doi.org/10.5194/hess-25-2353-2021

Sayers, P. B., Horritt, M., Carr, S., Kay, A., Mauz, J., Lamb, R., & Penning-Rowsell, E. (2020). *Third UK Climate Change Risk Assessment (CCRA3): Future flood risk*. Committee on Climate Change.

Schellekens, J., Van Verseveld, W., Visser, M., Winsemius, H., Euser, T., Bouaziz, L., Boisgontier, H., Thiange, C., De Vries, C., Eilander, D., Tollenaar, D., Hazenberg, P., Ten Velden, C. & et al. (2021). Openstreams/wow: Unstable-master. Available from https://github.com/openstreams/wflow.

Shortridge, J. E., & Zaitchik, B. F. (2018). Characterizing climate change risks by linking robust decision frameworks and uncertain probabilistic projections. *Climatic Change*, *151*, 525–539. https://doi.org/10.1007/s10584-018-2324-x

Sperna Weiland, F., Hegnauer, M., Bouaziz, L., & Beersma, J. J. (2015). *Implications of the KNMI'14 climate scenarios for the discharge of the Rhine and Meuse; comparison with earlier scenario studies*. Deltares.

Sperna Weiland, F. C., van Beek, L. P. H., Kwadijk, J. C. J., & Bierkens, M. F. P. (2012). Global patterns of change in discharge regimes for 2100. *Hydrology and Earth System Sciences*, *16*, 1047–1062. https://doi.org/10.5194/hess-16-1047-2012

Stahl, K., Weiler, M., Freudiger, D., Kohn, I., Seibert, J., Vis,M., Gerlinger,K., & Böhm, M. (2017) *The snow and glacier melt components of the streamflow of the River Rhine and its tributaries considering the influence of climate change*. International Commission for the Hydrology of the Rhine basin (CHR).

Sterl, A., van den Brink, H., de Vries, H., Haarsma, R., & van Meijgaard, E. (2009). An ensemble study of extreme storm surge related water levels in the North Sea in a changing climate. *Ocean Science*, *5*, 369–378. https://doi.org/10.5194/os-5-369-2009

Te Linde, A. H., Bubeck, P., Dekkers, J. E. C., de Moel, H., & Aerts, J. C. J. H. (2011). Future flood risk estimates along the river Rhine. *Natural Hazards and Earth System Sciences*, *11*, 459–473. https://doi.org/10.5194/nhess-11-459-2011

Themeßl, M. J., Gobiet, A., & Heinrich, G. (2012). Empirical-statistical downscaling and error correction of regional climate models and its impact on the climate change signal. *Climatic Change*, *112*(2), 449–468.

Van Alphen, J. (2016). The Delta Programme in The Netherlands. *Journal of Flood Risk Management*, *9*, 310–319. https://doi.org/10.1111/jfr3.12183

van den Hurk, B., van Meijgaard, E., de Valk, P., van Heeringen, K.-J., & Goijer, J. (2015). Analysis of a compounding surge and precipitation event in The Netherlands. *Environmental Research Letters*, *10*, 035001.

Van der Wiel, K., Wanders, N., Selten, F. M., & Bierkens, M. F. P. (2019). Added value of large ensemble simulations for assessing extreme river discharge in a 2 °C warmer world. *Geophysical Research Letters*, *46*, 2093–2102. https://doi.org/10.1029/2019GL081967

van Osnabrugge, B., Uijlenhoet, R., & Weerts, A. (2018). Contribution of potential evaporation forecasts to 10-day streamflow forecast skill for the Rhine river. *Hydrology and Earth System*

*Sciences*, *23*, 1453–1467. https://doi.org/10.5194/hess-23-1453-2019

van Osnabrugge, B., Weerts, A., & Uijlenhoet, R. (2017). genRE: A method to extend gridded precipitation climatology data sets in near real-time for hydrological forecasting purposes. *Water Resources Research*, *53*, 9284–9303. https://doi.org/10.1002/2017WR021201

Van Vuuren, D. P., Edmonds, J., Mikiko, K., Keywan, R., Thomson, A., Hibbard, K., Hurtt, G., Kram, T., Krey, V., Lamarque, J.-F., Masui, T., Meinshausen, M., Nakicenovic, N., Smith, S. J., & Rose, S. K. (2011). The representative concentration pathways: An overview. *Climatic Change*, *5*, 109–131. https://doi.org/10.1007/s10584-011-0148-z

Vorogushyn, S., Merz, B., & Apel, H. (2009). Development of dike fragility curves for piping and micro-instability breach mechanisms. *Natural Hazards and Earth System Sciences*, *9*, 1383–1401. https://doi.org/10.5194/nhess-9-1383-2009

Ward, P. J., Beets, W., Bouwer, L. M., & Aerts, J. C. J. H. (2010). Sensitivity of river discharge to ENSO. *Geophysical Research Letters*, *37*, L12402. https://doi.org/10.1029/2010GL043215

Ward, P. J., Van Pelt, S. C., De Keizer, O., Aerts, J. C. J. H., Beersma, J. J., Van den Hurk, B. J. J. M., & Te Linde, A. H. (2012). Including climate change projections in probabilistic flood risk assessment. *Journal of Flood Risk Management*, *7*(2), 141–151. https://doi.org/10.1111/jfr3.12029

Warren, R., Watkiss, P., Wilby, RL., Humphrey, K., Ranger, N., Betts, R., Lowe, J. & Watts, G. (2016) *UK climate change risk assessment evidence report: Chapter 2, approach and context*. (Report prepared for the adaptation sub-Committee of the Committee on climate change).

Whitfield, P. (2012). Changing floods in future climates. *Journal of Flood Risk Management*, *5*, 336–365. https://doi.org/10.1111/j.1753-318X.2012.01150.x

Wilcke, R. A. I., & Bärring, L. (2016). Selecting regional climate scenarios for impact modelling studies. *Environmental Modelling & Software*, *78*, 191–201. https://doi.org/10.1016/j.envsoft.2016.01.002

Willkofer, F., Schmid, F.-J., Komischke, H., Korck, J., Braun, M., & Ludwig, R. (2018). The impact of bias correcting regional climate model results on hydrological indicators for Bavarian catchments. *Journal of Hydrology: Regional Studies*, *19*, 25–41. https://doi.org/10.1016/j.ejrh.2018.06.010

Winsemius, H. C., Van Beek, L. P. H., Jongman, B., Ward, P. J., & Bouwman, A. (2013). A framework for global river flood risk assessments. *Hydrology and Earth System Sciences*, *17*, 1871–1892. https://doi.org/10.5194/hess-17-1871-2013

WMO. (2017). *WMO guidelines on the calculation of climate normals*. WMO No. 1203.

Zampieri, M., Scoccimarro, E., Gualdi, S., & Navarra, A. (2015). Observed shift towards earlier spring discharge in the main alpine rivers. *Science of the Total Environment*, *503–504*, 222–232. https://doi.org/10.1016/j.scitotenv.2014.06.036

Zhu, F., Emile-Geay, J., McKay, N. P., Hakim, G. J., Khider, D., Ault, T. R., Steig, E. J., Dee, S., & Kirchner, J. W. (2019). Climate models can correctly simulate the continuum of global-average temperature variability. *Proceedings of the National Academy of Sciences of the United States of America*, *116*(18), 8728–8733. https://doi.org/10.1073/pnas.1809959116

**How to cite this article:** Sperna Weiland, F., Stuparu, D., de Winter, R., & Haasnoot, M. (2022). Improving hydrological climate impact assessments using multirealizations from a global climate model. *Journal of Flood Risk Management*, *15*(2), e12787. https://doi.org/10.1111/jfr3.12787